Perfect Boundary Conditions for Parabolic Water-Wave Models

by

Robert A. Dalrymple and P. A. Martin

RESEARCH REPORT NO. CACR-91-08

August, 1991

CENTER FOR APPLIED COASTAL RESEARCH

DEPARTMENT OF CIVIL ENGINEERING
UNIVERSITY OF DELAWARE
NEWARK, DELAWARE 19716

Perfect boundary conditions for parabolic water-wave models

BY ROBERT A. DALRYMPLE[1] AND P. A. MARTIN[2]

[1] *Center for Applied Coastal Research, Department of Civil Engineering University of Delaware, Newark, DE 19716, U.S.A.*

[2] *Department of Mathematics, University of Manchester Manchester M13 9PL, U.K.*

Generalized impedance boundary conditions are presented for parabolic wave models, which provide either perfect diffractive boundary conditions or perfect transmitting boundary conditions. The diffractive conditions permit the modelling of waves in illuminated regions without computations in the shadow regions, while the transmitting conditions allow incident and scattered waves to propagate out of the model. The theory is developed for the simplest parabolic model and for a class of wide-angle parabolic models. Numerical results are presented.

1 Introduction

The propagation of water waves over a three-dimensional ocean is governed by Laplace's equation, an elliptic partial differential equation. As the solution of such equations over large domains is computationally intensive, parabolic approximations have been developed; see, for example, Radder (1979), Mei & Tuck (1980), Booij (1981), Tsay & Liu (1982) and Kirby & Dalrymple (1983). These approximations are appropriate when the waves propagate mainly in one direction, taken to be the x-direction, and lead to parabolic partial differential equations; these can be solved numerically by marching in x.

The development of parabolic wave models for water-wave propagation over large coastal regions has lead to an interest in the associated model lateral boundary conditions, located, for example, at $y = 0$ and $y = y_b$. Here, x, y and z are Cartesian coordinates, with $z = 0$ corresponding to the undisturbed free surface. The governing parabolic equation also requires an 'initial' condition at $x = 0$, say; a downwave condition is not required. Thus, the computational domain is the strip $x > 0$, $0 < y < y_b$. In this paper, we develop lateral boundary conditions that permit waves to leave the computational domain, regardless of their character (such as wave direction or crest curvature).

1.1 *Parabolic models*

To establish the mathematical framework for the lateral boundary conditions, the simplest parabolic model will be briefly derived. We consider the irrotational motion of an

incompressible, inviscid fluid. The velocity potential ϕ satisfies the three-dimensional Laplace equation. Write it as

$$\phi(x,y,z,t) = \mathrm{Re}\left\{ A(x,y)\frac{\cosh k(h+z)}{\cosh kh}\,\mathrm{e}^{\mathrm{i}(kx-\omega t)} \right\}, \tag{1.1}$$

where the bottom is located at $z = -h$ ($h > 0$); the wavenumber k and the wave angular frequency ω are related by the dispersion relation,

$$\omega^2 = gk \tanh kh,$$

where g is the acceleration due to gravity. Assuming that h is constant, we can obtain a parabolic equation by substituting the assumed form (1.1) into Laplace's equation and then discarding a term proportional to $\partial^2 A/\partial x^2$. This may be justified by supposing that $A(x,y)$ is a slowly-varying function of x, whence

$$\left|\frac{\partial A}{\partial x}\right| \ll |kA|. \tag{1.2}$$

The resulting equation is

$$2\mathrm{i}k\,\frac{\partial A}{\partial x} + \frac{\partial^2 A}{\partial y^2} = 0. \tag{1.3}$$

We call (1.3) the *simple parabolic equation*. A generalization of (1.3) is

$$2\mathrm{i}k\,\frac{\partial A}{\partial x} + 2\alpha\,\frac{\partial^2 A}{\partial y^2} + \frac{2\mathrm{i}\beta}{k}\,\frac{\partial^3 A}{\partial x \partial y^2} = 0, \tag{1.4}$$

where α and β are positive constants. We call (1.4) the *wide-angle parabolic equation*; it was discussed by Kirby (1986*a*), wherein $a_0 = 1$, $a_1 = -\alpha - \beta$ and $b_1 = -\beta$. Note that (1.4) reduces to (1.3) when $\alpha = \frac{1}{2}$ and $\beta = 0$, whereas (1.4) reduces to 'Claerbout's equation' when $\alpha = \frac{1}{2}$ and $\beta = \frac{1}{4}$ (Claerbout 1976, pp. 206–207). In practice, parabolic models are often more elaborate than (1.3) and (1.4); variable depth, currents and, in some cases, wave nonlinearity may be included.

Parabolic approximations are also used widely for underwater acoustics, in which sound waves propagate through a compressible ocean. For a review, see Ames & Lee (1987). If the speed of sound in the ocean is taken to be constant, equations such as (1.3) and (1.4) are obtained.

1.2 *Lateral boundary conditions*

One solution of (1.3) is

$$A(x,y) = A_0\,\mathrm{e}^{-\frac{1}{2}\mathrm{i}kx\sin^2\theta}\mathrm{e}^{\mathrm{i}k(y-y_b)\sin\theta}, \tag{1.5}$$

corresponding to a plane wave propagating at an angle θ to the x-axis (A_0 is a constant). For the case of reflection from a lateral boundary at $y = y_b$, we can write the total solution as

$$A(x,y) = A_0\,\mathrm{e}^{-\frac{1}{2}\mathrm{i}kx\sin^2\theta}\left(\mathrm{e}^{\mathrm{i}k(y-y_b)\sin\theta} + R\,\mathrm{e}^{-\mathrm{i}k(y-y_b)\sin\theta}\right), \tag{1.6}$$

where R is the (complex) reflection coefficient; $|R|$ can vary between zero and unity depending on the amount of reflection from the boundary.

At present, a typical application of a parabolic model (such as (1.3)) requires a very wide domain such that the influence of the lateral boundary conditions are far away from the region of interest, hence not introducing any contamination due to an imperfect boundary condition. This of course means that far more numerical computation is carried out than is desired. Efficient lateral boundary conditions would mean that model computations would only include the region of interest.

There are two problems of interest, namely diffraction and transmission. More precisely, divide the first quadrant into an 'illuminated region' ($x > 0$, $0 < y < y_b$) and a 'shadow region' ($x > 0$, $y > y_b$). For a *diffraction problem*, suppose that there is a semi-infinite breakwater along $x = 0$, $y > y_b$ (where A vanishes) and waves are incident from the region $x < 0$; see figure 1. At present, computations would include both the shadow region and the illuminated region. If only the illuminated region is of interest, we could reduce the computational domain immensely by placing a suitable 'diffractive' boundary condition along the interface between the two regions, namely $x > 0$, $y = y_b$; see §3.1. For a *transmission problem*, we allow waves to pass cleanly through the line $x = 0$, $y > y_b$ (along which A does not vanish, in general). In order to reduce the computational domain to the illuminated region, we now place a suitable 'transmitting' boundary condition along $x > 0$, $y = y_b$; see §3.2. (In practice, we will always impose one of the new boundary conditions along a line parallel to the x-axis, even for obliquely incident wave trains.)

The lateral boundary condition usually employed in a parabolic model is an impedance boundary condition. The impedance, $\mathcal{Z}$, in our context, is defined as the ratio of pressure at the boundary to normal velocity at the boundary,

$$\mathcal{Z} = \frac{\left(\rho \frac{\partial \phi}{\partial t}\right)}{\left(-\frac{\partial \phi}{\partial y}\right)} = \frac{\mathrm{i}\omega\rho\phi}{\left(\frac{\partial \phi}{\partial y}\right)} \quad \text{on } y = y_b. \tag{1.7}$$

For our plane-wave solution with reflection, (1.6), we have

$$\mathcal{Z} = \frac{\rho\omega}{k \sin\theta} \frac{(1+R)}{(1-R)} \tag{1.8}$$

showing that the impedance of the boundary depends on the angle of incidence and the reflection coefficient; neither of these is necessarily known.

Rewriting (1.7), using (1.1), we have the impedance boundary condition

$$\frac{\partial A}{\partial y} - \frac{\mathrm{i}\rho\omega}{\mathcal{Z}} A = 0 \quad \text{on } y = y_b. \tag{1.9}$$

In general, $\mathcal{Z}$ could be real or complex. A real value of the impedance will lead to transmission of waves and wave energy. A purely imaginary value will result in a phase shift of the reflected wave, but no transmission. A complex $\mathcal{Z}$ results in transmission and reflection.

For example, for plane waves with the impedance given as (1.8), the impedance boundary condition becomes

$$\frac{\partial A}{\partial y} - \mathrm{i}k \sin\theta \, \frac{(1-R)}{(1+R)} A = 0 \quad \text{on } y = y_b. \tag{1.10}$$

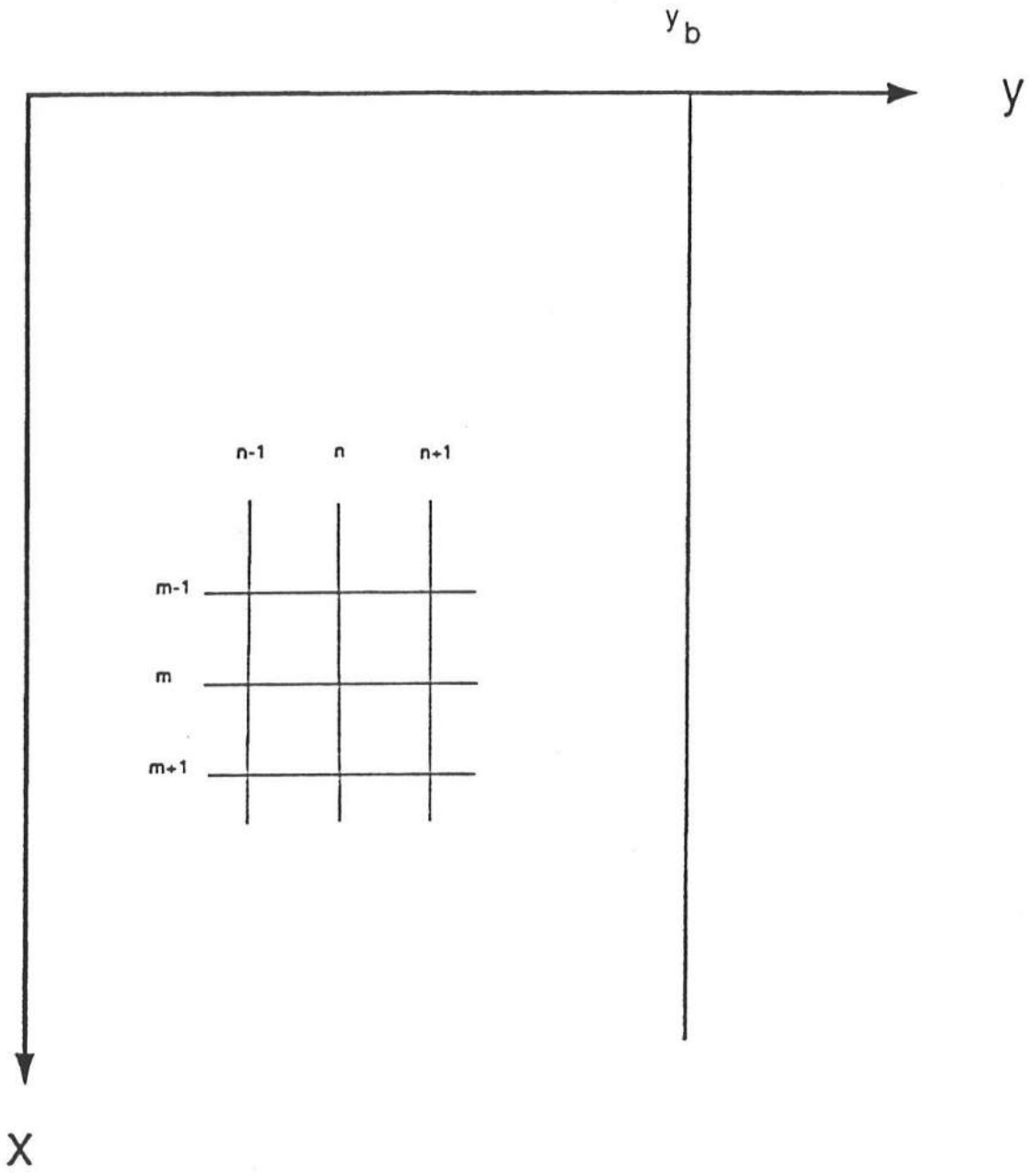

Figure 1: A sketch of the computational domain ($x > 0$, $0 < y < y_b$) and the analytical domain ($x > 0$, $y > y_b$). A piece of the computational mesh is also shown.

For a perfectly reflecting boundary, R is set to unity. For a perfectly transmitting boundary condition, R is set to zero, yielding

$$\frac{\partial A}{\partial y} - ik \sin\theta \, A = 0 \quad \text{on } y = y_b. \tag{1.11}$$

This boundary condition requires, in addition to planar wave trains at the boundary, that both k and the wave angle, θ be known at the boundary. These parameters can be difficult to obtain within a computational model. One possibility is to assume that $\sin\theta = 1$, leading to a simplification. However, as Behrendt (1984) has shown (see also Kirby, 1989), this leads to a reflection coefficient,

$$R = \frac{\sin\theta - 1}{\sin\theta + 1}, \tag{1.12}$$

which is only zero for $\theta = 90°$ (waves at normal incidence to the boundary) and reaches a value -1 for $\theta = 0$ (grazing incidence).

Alternatively, Kirby (1986*b*) numerically implemented the lateral boundary condition (1.11), for waves propagating over a variable-depth domain. The condition assumes that the longshore wavenumber, $k \sin\theta$, is calculable from the previous computational grid row. Kirby states that this condition can be used on the upwave or downwave lateral boundary, but should be far from scattering objects within the model domain, as scattering of waves occurring within the computational domain will be partially reflected by this 'plane-wave' boundary condition. The intention of this practice is to have the weak reflection enter the computational domain downwave of the area of interest.

Finally, 'sponge-layer' models have been introduced, which involve regions of high energy dissipation near the side walls of the computational domain (Israeli & Orszag, 1981; Larsen & Dancy, 1983). The sponge layers serve as absorbing boundaries, with the disadvantage of additional computational domain, diffraction into the boundaries, and weak reflection. By placing these boundaries far from the region of interest, suitable solutions may be obtained.

Here, generalized impedance boundary conditions will be developed to permit waves to exit the domain regardless of the wave direction, crest curvature, or strength of scattering. The method closely follows that of Marcus (1991), developed to produce transmitting boundary conditions for underwater acoustics. As will be shown, the method works for diffracting as well as transmitting boundaries. A comparison with Kirby's plane-wave boundary condition is also provided in the numerical examples. The method is extended so as to treat the wide-angle equation (1.4).

2 Numerical representation of the simple parabolic model

Before developing the boundary condition, we discuss the discretization of the simple parabolic equation (1.3) and its solution using the Crank-Nicolson scheme to provide the numerical framework for what follows; the wide-angle equation (1.4) is considered in §5. We superimpose a regular mesh on the computational domain $x > 0$, $0 < y < y_b$, with grid points at (x_m, y_n), where $x_m = m\Delta x$, $y_n = (n - \frac{1}{2})\Delta y$, $m = 0, 1, 2, \ldots, M$ and

$n = 0, 1, 2, \ldots, N$. By construction, $y_b = (N-1)\Delta y$. Denote

$$A_n^m = A(x_m, y_n).$$

The Crank-Nicolson approach, which is an implicit scheme with second-order accuracy in both Δx and Δy, is written as

$$2ik\left(\frac{A_n^m - A_n^{m-1}}{\Delta x}\right) + \frac{1}{2}\left\{\frac{A_{n+1}^m - 2A_n^m + A_{n-1}^m}{(\Delta y)^2} + \frac{A_{n+1}^{m-1} - 2A_n^{m-1} + A_{n-1}^{m-1}}{(\Delta y)^2}\right\} = 0.$$

This scheme is consistent and stable. It is also convenient in that it uses only the results from row $m-1$ to compute row m, resulting in a tridiagonal matrix when applied to all of the n values excluding those on the boundary. Boundary conditions have to be applied at $n = 0$ and $n = N$ to provide enough equations to solve for the unknowns, A_n^m, $n = 0, 1, 2, \ldots, N$. Once these conditions are included, the resulting equations may be solved using a (complex) tridiagonal solver; these are very fast. An analysis of the numerical scheme (in fact. for the wide-angle parabolic equation (1.4) in the context of underwater acoustics) has been given by St. Mary & Lee (1985).

In finite-difference form, the transmitting boundary condition used by Kirby (1986*b*) is

$$\frac{A_{n+1}^m - A_n^m}{\Delta y} - ik\sin\theta\left(\frac{A_{n+1}^m + A_n^m}{2}\right) = 0 \quad \text{for } n = 0 \text{ or } n = N-1, \tag{2.1}$$

when the boundary is located at $y = 0$ or $y = y_b$, respectively. The longshore wavenumber component, $k\sin\theta$, is found by evaluating (2.1) at the previous grid row:

$$k\sin\theta = -\frac{2\mathrm{i}}{\Delta y}\frac{\left(A_{n+1}^{m-1} - A_n^{m-1}\right)}{\left(A_{n+1}^{m-1} + A_n^{m-1}\right)}. \tag{2.2}$$

Kirby shows that this condition, (2.1) with (2.2), is exact for plane waves.

3 Theoretical development of the boundary conditions

The basis for the boundary condition is the exact description of the waves in the shadow region (outside of the computational domain); denote the solution in this region by $\mathcal{A}(x, y)$. Denote the solution in the computational domain (the illuminated region) by $A(x, y)$. These two solutions must match across the interface $y = y_b$,

$$A(x, y_b) = \mathcal{A}(x, y_b) \qquad \text{and} \qquad \frac{\partial A(x, y_b)}{\partial y} = \frac{\partial \mathcal{A}(x, y_b)}{\partial y}. \tag{3.1}$$

Now, it is shown in the Appendix that, for diffraction problems (§1.2), $\mathcal{A}$ is given by (A 8) as

$$\mathcal{A}(x, y) = -\frac{1}{2}\mathrm{i}(y - y_b)\Omega\int_0^x \frac{\mathcal{A}(\xi, y_b)}{(x-\xi)^{3/2}}\exp\left\{\frac{ik(y-y_b)^2}{2(x-\xi)}\right\}d\xi$$

for $y \geq y_b$, where $\Omega = \sqrt{(2ik/\pi)} = (1+\mathrm{i})\sqrt{(k/\pi)}$. Although this formula shows that $\mathcal{A}(x, y)$ depends solely on values of $\mathcal{A}(\xi, y_b)$ for $\xi \leq x$, it is not easy to use within our

numerical scheme. Instead, following Marcus (1991), we differentiate with respect to y to give (A 9), namely

$$\frac{\partial A(x,y)}{\partial y} = \mathrm{i}\Omega \int_0^x \frac{\partial A(\xi,y)}{\partial \xi} \frac{d\xi}{\sqrt{x-\xi}}.$$

If we set $y = y_b$ and use the matching conditions (3.1), we obtain

$$\frac{\partial A(x,y_b)}{\partial y} = \mathrm{i}\Omega \int_0^x \frac{\partial A(\xi,y_b)}{\partial \xi} \frac{d\xi}{\sqrt{x-\xi}}. \tag{3.2}$$

The formula (3.2) is exact. It shows that the condition to be imposed on $y = y_b$ is *not* an impedance condition of the form (1.9). However, we will show that when (3.2) is discretised, it leads to a condition that is similar to an inhomogeneous impedance condition; it is called a *generalized impedance boundary condition.*

From (3.2), we have

$$\frac{\partial A_b^m}{\partial y} = \mathrm{i}\Omega \int_0^{x_m} \frac{\partial A(\xi,y_b)}{\partial \xi} \frac{d\xi}{\sqrt{x_m-\xi}},$$

where $A_b^m = A(x_m, y_b)$. We assume that $A(\xi, y_b)$ is approximated by a continuous piecewise-linear function, so that

$$\frac{\partial A(\xi,y_b)}{\partial \xi} = \frac{A_b^{l+1} - A_b^l}{\Delta x} \quad \text{for } x_l < \xi < x_{l+1}. \tag{3.3}$$

Hence

$$\frac{\partial A_b^m}{\partial y} = \sum_{l=0}^{m-1} (A_b^{l+1} - A_b^l)\, L_l(x_m), \tag{3.4}$$

where

$$L_l(x) = \frac{\mathrm{i}\Omega}{\Delta x} \int_{x_l}^{x_{l+1}} \frac{d\xi}{\sqrt{x-\xi}} = \frac{2\mathrm{i}\Omega}{\Delta x} \left(\sqrt{x-x_l} - \sqrt{x-x_{l+1}} \right),$$

whence

$$L_l(x_m) = \frac{2\mathrm{i}\Omega}{\sqrt{\Delta x}} \left(\sqrt{m-l} - \sqrt{m-l-1} \right).$$

Rearranging (3.4), we have

$$\begin{aligned} \frac{\partial A_b^m}{\partial y} - A_b^m L_{m-1}(x_m) &= -A_b^{m-1} L_{m-1}(x_m) + \sum_{l=0}^{m-2} (A_b^{l+1} - A_b^l)\, L_l(x_m) \\ &= \sum_{l=1}^{m-1} A_b^l \{ L_{l-1}(x_m) - L_l(x_m) \} - A_b^0 L_0(x_m). \end{aligned}$$

If we substitute for $L_l(x_m)$, we obtain

$$\frac{\partial A_b^m}{\partial y} + a A_b^m = \sum_{l=0}^{m-1} b_l^m A_b^l \tag{3.5}$$

as our generalized impedance boundary condition on $y = y_b$, where

$$\begin{aligned} a &= -\frac{2\mathrm{i}\Omega}{\sqrt{\Delta x}}, \\ b_0^m &= -\frac{2\mathrm{i}\Omega}{\sqrt{\Delta x}} \left(\sqrt{m} - \sqrt{m-1} \right), \\ b_l^m &= -\frac{2\mathrm{i}\Omega}{\sqrt{\Delta x}} \left(2\sqrt{m-l} - \sqrt{m-l-1} - \sqrt{m-l+1} \right), \quad \text{for } l = 1, 2, \ldots, m-1. \end{aligned}$$

3.1 *The diffractive boundary condition*

The analysis above is appropriate when the lateral boundary at $y = y_b$ divides an illuminated region ($y < y_b$), where the wave field will be calculated numerically, and a shadow region ($y > y_b$) into which the waves are diffracting. We call the corresponding condition on $y = y_b$ the *diffractive boundary condition*. It is implemented into the parabolic model by recalling that this boundary is at $y = \frac{1}{2}(y_{N-1} + y_N)$; thus, we use central differences and averages to approximate $\partial A_b^m/\partial y$ and A_b^m, respectively. The result is

$$\frac{A_N^m - A_{N-1}^m}{\Delta y} + \frac{a}{2}\left(A_N^m + A_{N-1}^m\right) = \frac{1}{2}\sum_{l=0}^{m-1} b_l^m (A_N^l + A_{N-1}^l). \tag{3.6}$$

This is the diffractive boundary condition; it is used for $n = N$ in the matrix formulation of the problem.

3.2 *The transmitting boundary condition*

Suppose that we have a transmission problem (§1.2) with a known incident wave field $A_{\text{inc}}(x, y)$; in general, $A_{\text{inc}}(0, y)$ does not vanish identically for $y > y_b$. Let us perturb the incident field within the computational domain ($y < y_b$), so that the total field is $A(x, y)$. The difference,

$$A - A_{\text{inc}} = A_s, \tag{3.7}$$

say, will satisfy $A_s(0, y) = 0$ for $y > y_b$, and hence will solve the same mathematical problem in the shadow region as A. Thus,

$$\frac{\partial A_s(x, y_b)}{\partial y} = \mathrm{i}\Omega \int_0^x \frac{\partial A_s(\xi, y_b)}{\partial \xi} \frac{d\xi}{\sqrt{x - \xi}}. \tag{3.8}$$

It follows that we can derive a boundary condition for A_s on $y = y_b$ by discretisation, as for the diffractive boundary condition.

In practice, a boundary condition for A is often preferable. Combining (3.7) and (3.8), we obtain

$$\frac{\partial A(x, y_b)}{\partial y} = \mathrm{i}\Omega \int_0^x \frac{\partial A(\xi, y_b)}{\partial \xi} \frac{d\xi}{\sqrt{x - \xi}} + F_{\text{inc}}(x), \tag{3.9}$$

where

$$F_{\text{inc}}(x) = \frac{\partial A_{\text{inc}}(x, y_b)}{\partial y} - \mathrm{i}\Omega \int_0^x \frac{\partial A_{\text{inc}}(\xi, y_b)}{\partial \xi} \frac{d\xi}{\sqrt{x - \xi}} \tag{3.10}$$

is known, in principle. If A_{inc} is only known numerically, (3.10) can be discretised as before. If A_{inc} is known analytically, further progress may be possible. For example, if A_{inc} is given by (1.5), we have

$$F_{\text{inc}}(x) = A_0 \mathrm{i}k \sin\theta\, \mathrm{e}^{-2\mathrm{i}\kappa x} - 2A_0\Omega\kappa \int_0^x \frac{\mathrm{e}^{-2\mathrm{i}\kappa\xi}}{\sqrt{x - \xi}}\, d\xi,$$

where $\kappa = \frac{1}{4}k\sin^2\theta$. Denote the integral by I; it can be evaluated by putting $\xi = x\sin^2(\varphi/2)$, so that

$$\begin{aligned} I &= \sqrt{x}\mathrm{e}^{-2\mathrm{i}\kappa x} \int_0^\pi \mathrm{e}^{\mathrm{i}\kappa x\cos\varphi} \sin(\varphi/2)\, d\varphi \\ &= \sqrt{x}\mathrm{e}^{-2\mathrm{i}\kappa x} \sum_{n=0}^{\infty} \varepsilon_n \mathrm{i}^n J_n(\kappa x) \int_0^\pi \cos n\varphi \sin(\varphi/2)\, d\varphi, \end{aligned}$$

where $J_n(x)$ is a Bessel function, $\varepsilon_0 = 1$ and $\varepsilon_n = 2$ for $n > 0$. Hence

$$F_{\text{inc}}(x) = A_0 e^{-2i\kappa x} \left\{ ik \sin\theta + 4\Omega\kappa\sqrt{x} \sum_{n=0}^{\infty} \frac{\varepsilon_n i^n}{4n^2 - 1} J_n(\kappa x) \right\}.$$

In summary, we have two alternative transmitting boundary conditions, one for A_s (the change in A_{inc} due to any scattering from the computational domain) and one for A (the total field, namely the sum of A_{inc} and A_s).

4 Results

To illustrate the use of the generalized boundary conditions, a numerical model was set up with Kirby's transmitting condition (2.1) at $y = 0$ and a generalized boundary condition at $y = y_b$ (for all cases). The model grid is 100×100 and the grid sizes are $k\Delta x = k\Delta y = 0.622$, or about ten grid points per wavelength. The constant relative water depth, kh, is arbitrarily taken as 1.037. In all the figures, the x-axis points downwards and the y-axis points to the right.

The first test of the model is for plane waves, defined by (1.5); we render quantities dimensionless by taking $A_0 = 1$. The waves propagate at $\theta = 20°$ to the x-axis. We take the transmitting boundary condition (3.9) and evaluate F_{inc} numerically from (3.10). The initial values of A are provided to the model by

$$A(0, y) = e^{iky \sin\theta} \quad 0 < y < y_b.$$

Figure 2 shows the resulting instantaneous wave height (actually $\text{Re}\{A(x, y)e^{ikx}\}$) from the parabolic model. Clearly the waves transmit through both of the boundaries correctly.

Next, for $\theta = 0$, a disturbance is introduced at $x = 0$ by arbitrarily reducing the amplitude over seven grid locations, located at the centre of the grid, using the following weights (0.9, 0.8, 0.6, 0.5, 0.6, 0.8, 0.9). In figure 3, the absolute value of the wave amplitude $|A(x, y)|$ (or equivalently the transmission, or diffraction, coefficient) is shown in a grey scale; the numerical values are provided in a contour plot. Note that the solution is symmetric about the centreline, due to the symmetric initial disturbance, until the diffraction fringe from the disturbance reaches the boundaries. In this case, the perturbation reflects from the left boundary but is permitted to exit the computational domain by the generalized boundary condition on the right boundary.

In the last figures, a diffractive boundary condition is used on the right boundary. In figure 4, the transmission coefficient $|A(x, y)|$ is shown in grey scale. The diffractive fringes induced by the 'virtual' breakwater along the initial grid row but to the right of the computational domain are clearly shown. Further, they reflect from the left transmitting boundary and are transmitted by the right boundary. Along the right boundary, the transmission coefficient is 0.5, as expected by analytical results (Mei 1989, §10.7).

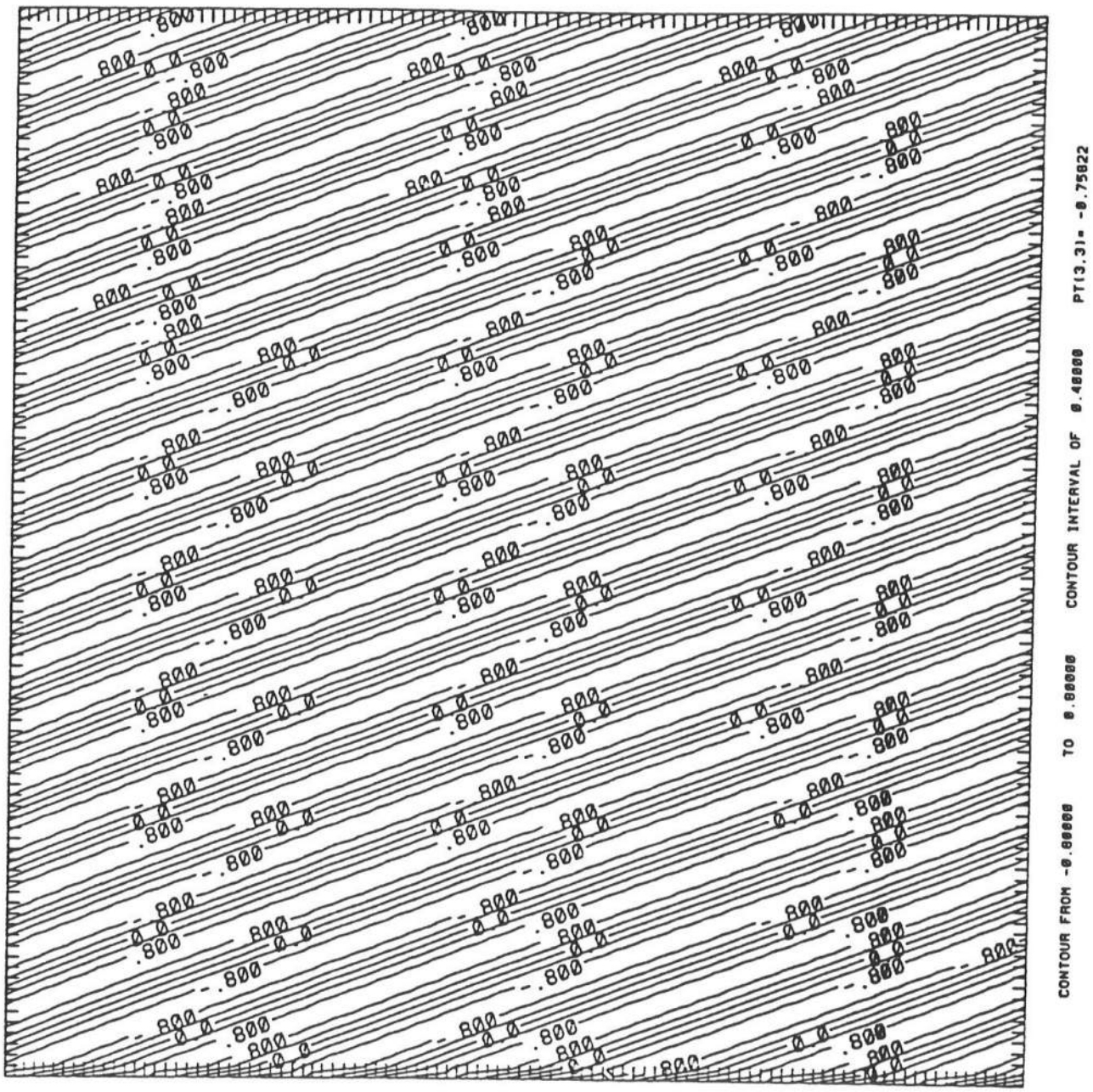

Figure 2: Transmission of a plane wave through both types of transmission boundary condition. Contours of instantaneous free-surface elevations.

(a)

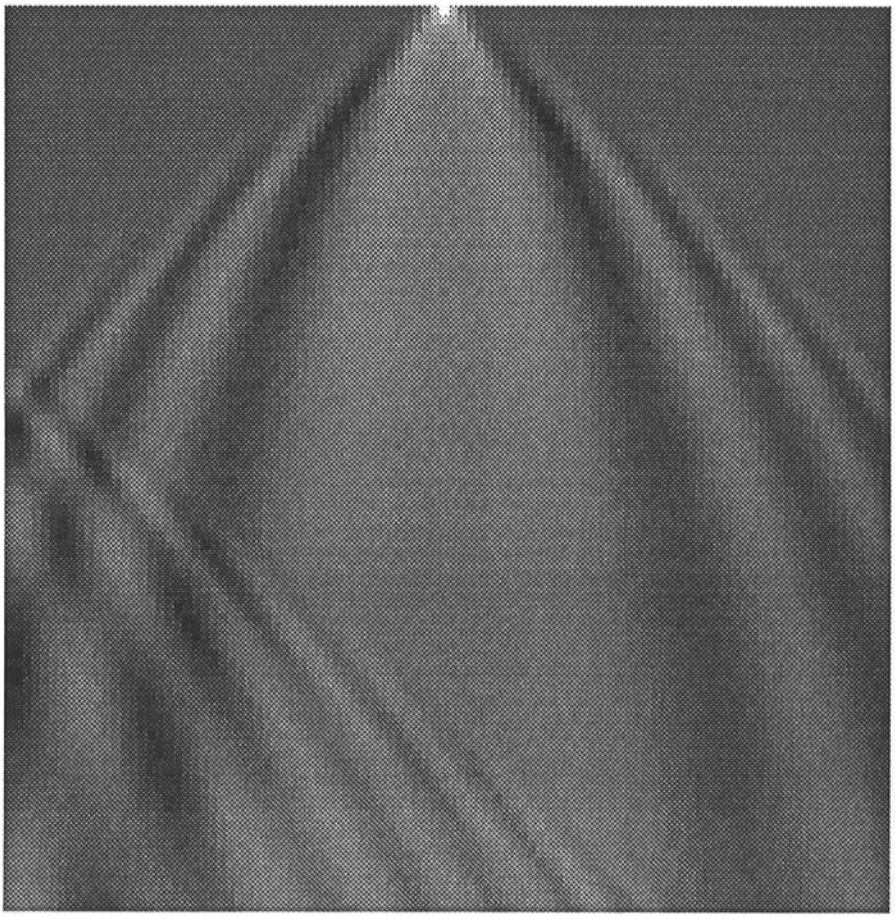

Figure 3: Transmission boundary conditions with a normally incident plane wave perturbed by an 'obstacle' on $x = 0$. In (a): density plot of transmission coefficient. In (b): contours of transmission coefficient.

(b)

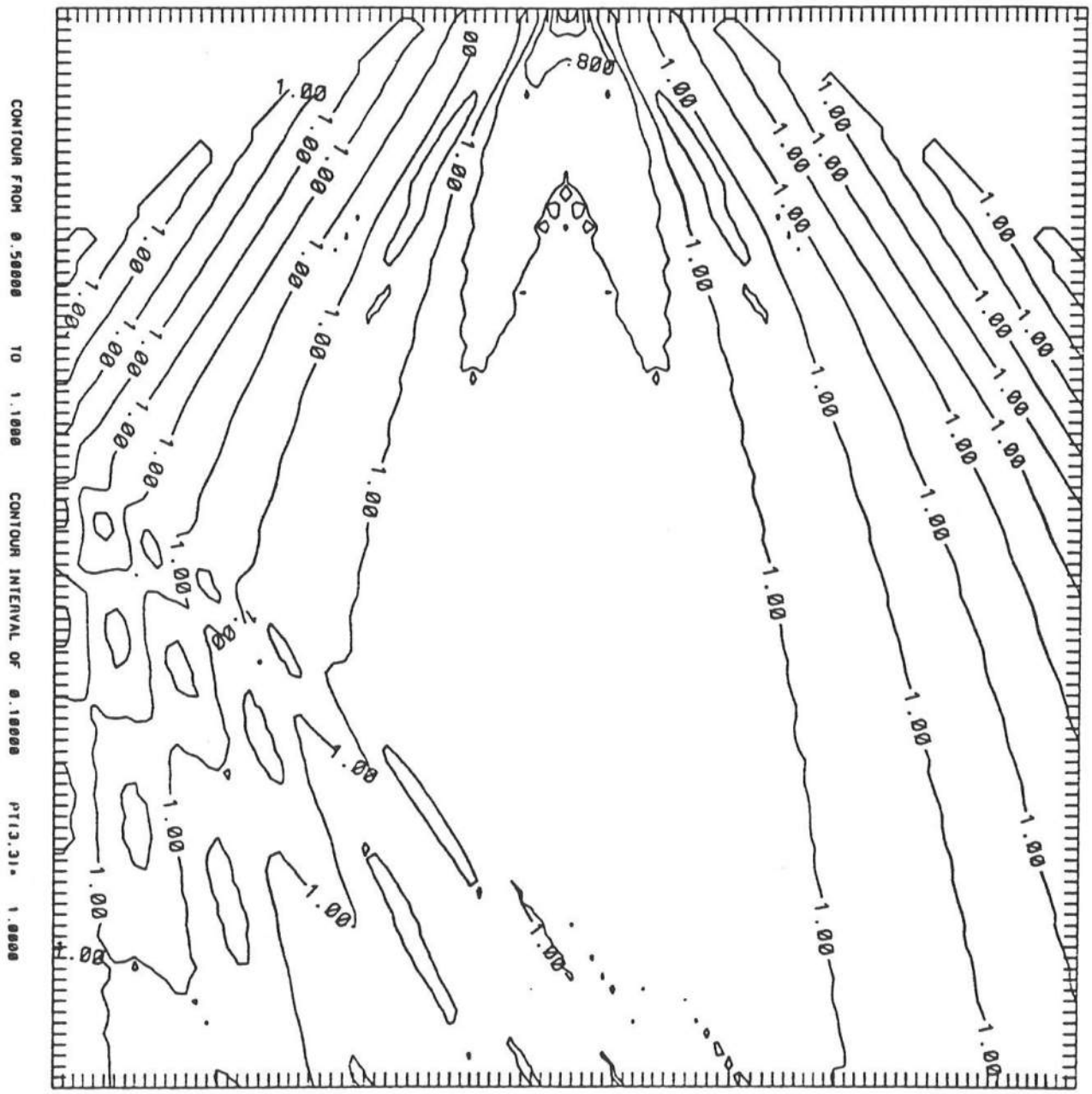

Figure 3: Transmission boundary conditions with a normally incident plane wave perturbed by an 'obstacle' on $x = 0$. In (a): density plot of transmission coefficient. In (b): contours of transmission coefficient.

(a)

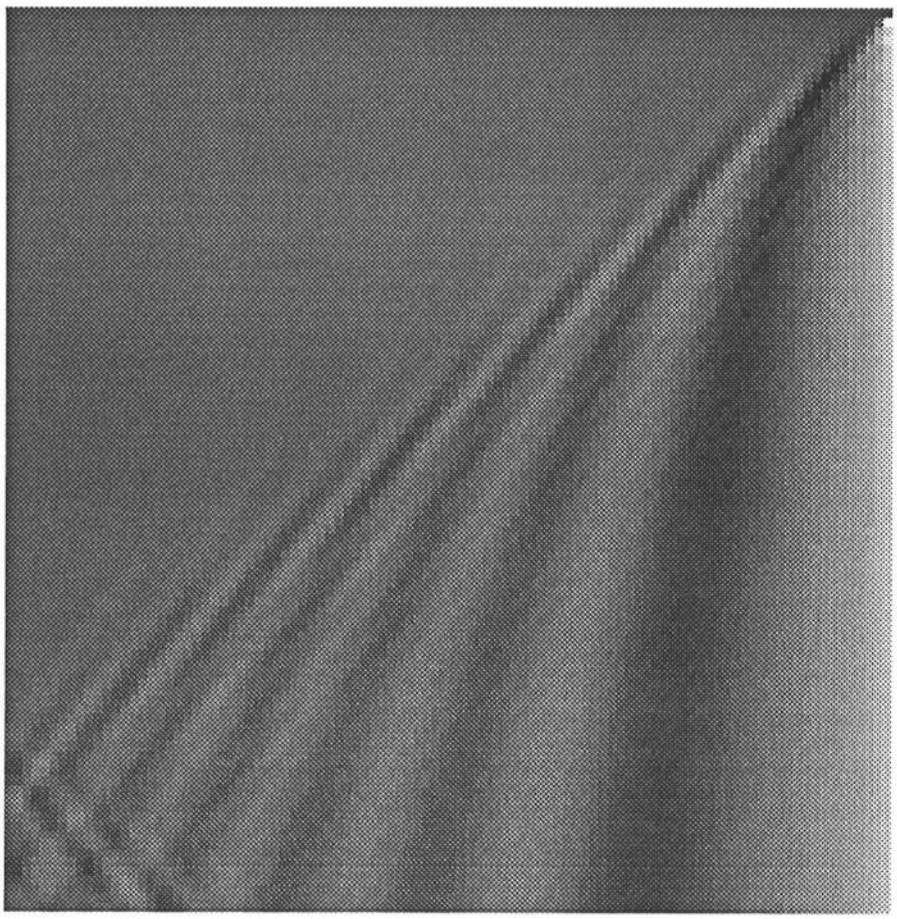

Figure 4: Transmission condition (on left boundary) and diffractive condition (on right boundary) with a normally incident plane wave. In (a): density plot of transmission coefficient. In (b): contours of transmission coefficient.

(b)

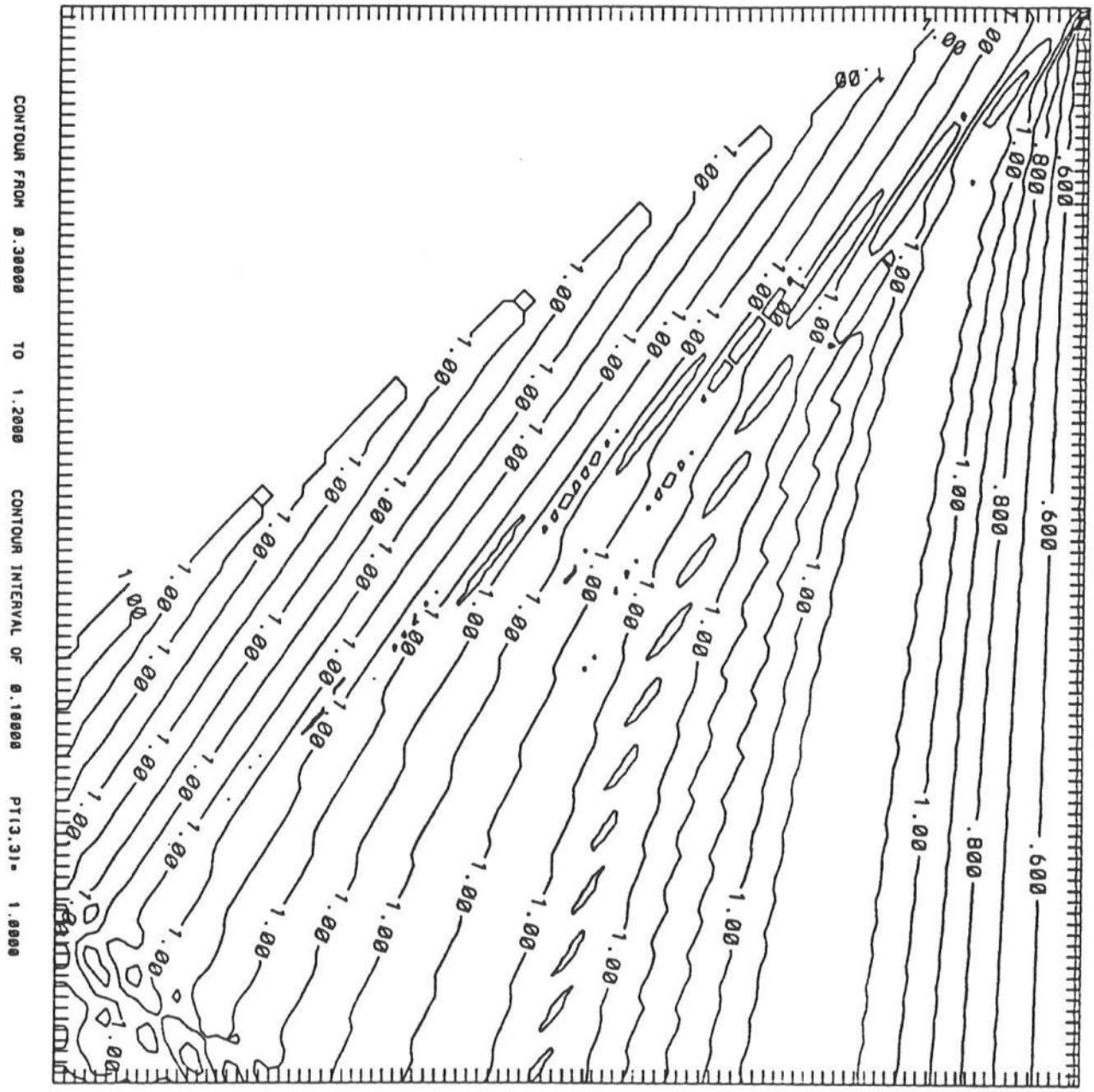

Figure 4: Transmission condition (on left boundary) and diffractive condition (on right boundary) with a normally incident plane wave. In (*a*): density plot of transmission coefficient. In (*b*): contours of transmission coefficient.

Lastly, a perturbation is once again introduced in the first row and the diffractive boundary condition is used. Again the scattering introduced by the perturbation is allowed to exit the domain by the generalized impedance boundary condition (figure 5).

5 The wide-angle parabolic equation

Consider the wide-angle parabolic equation, (1.4). This equation can also be discretised using the Crank-Nicolson scheme. In the Appendix, it is shown that the wave field in the shadow region is exactly modelled by (A 11), namely

$$\frac{\partial A(x,y_b)}{\partial y} = \frac{\mathrm{i}k}{\sqrt{\beta}} \int_0^x \mathrm{e}^{\mathrm{i}\lambda(x-\xi)} J_0(\lambda(x-\xi)) \frac{\partial A(\xi,y_b)}{\partial \xi}\, d\xi,$$

where

$$\lambda = \frac{k\alpha}{2\beta}.$$

If we discretise as before. using (3.3), we obtain

$$\frac{\partial A_b^m}{\partial y} - A_b^m L_{m-1}^\lambda(x_m) = \sum_{l=1}^{m-1} A_b^l \left\{ L_{l-1}^\lambda(x_m) - L_l^\lambda(x_m) \right\} - A_b^0 L_0^\lambda(x_m),$$

where

$$L_l^\lambda(x) = \frac{\mathrm{i}k}{\sqrt{\beta}\,\Delta x} \int_{x_l}^{x_{l+1}} \mathrm{e}^{\mathrm{i}\lambda(x-\xi)} J_0(\lambda(x-\xi))\, d\xi.$$

These integrals can be evaluated exactly, using the formula

$$Q(z) \equiv \int_0^z J_0(x)\, \mathrm{e}^{\mathrm{i}x}\, dx = z\mathrm{e}^{\mathrm{i}z} \left(J_0(z) - \mathrm{i}J_1(z)\right),$$

given by Gradshteyn & Ryzhik (1980, §6.674, Eqs. (7) & (8)). Hence

$$L_l^\lambda(x) = \frac{\mathrm{i}k}{\mu\sqrt{\beta}} \left\{ Q(\lambda(x-x_l)) - Q(\lambda(x-x_{l+1})) \right\},$$

where $\mu = \lambda\Delta x$. It follows that we have the generalized impedance boundary condition (3.5), where now

$$\begin{aligned}
a &= -\frac{\mathrm{i}k}{\sqrt{\beta}}\, \mathrm{e}^{\mathrm{i}\mu} \left\{ J_0(\mu) - \mathrm{i}J_1(\mu) \right\}, \\
b_0^m &= -\frac{\mathrm{i}k}{\mu\sqrt{\beta}} \left\{ Q(m\mu) - Q((m-1)\mu) \right\}, \\
b_l^m &= -\frac{\mathrm{i}k}{\mu\sqrt{\beta}} \left\{ 2Q((m-l)\mu) - Q((m-l+1)\mu) - Q((m-l-1)\mu) \right\},
\end{aligned}$$

for $l = 1, 2, \ldots, m-1$. We can now proceed to derive diffractive and transmitting boundary conditions, as before. We remark that the results of §3 can be recovered by setting $\alpha = \frac{1}{2}$ and letting $\lambda \to \infty$ ($\beta \to 0$), using the well-known large-argument approximations for Bessel functions; note that

$$Q(z) \sim \sqrt{\frac{2z}{\pi}}\, \mathrm{e}^{\mathrm{i}\pi/4} \quad \text{as } z \to \infty.$$

(a)

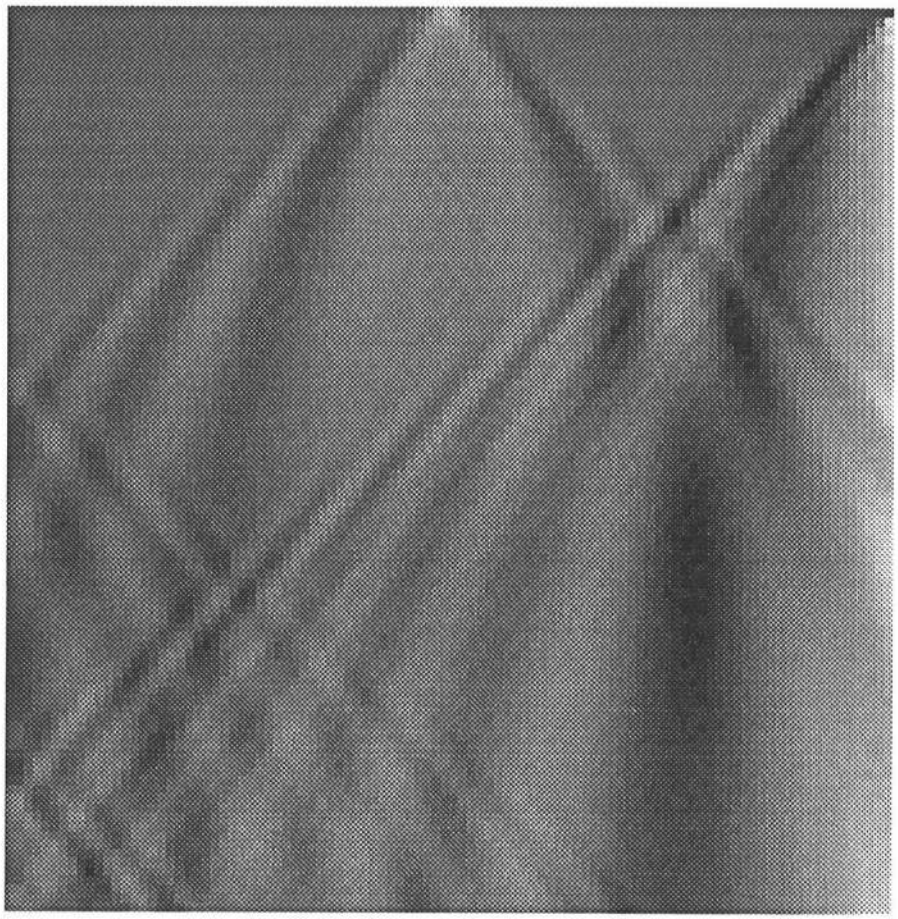

Figure 5: Transmission condition (on left boundary) and diffractive condition (on right boundary) with a normally incident plant wave perturbed by an 'obstacle' on $x = 0$. In (a): density plot of transmission coefficient. In (b): contours of transmission coefficient.

(b)

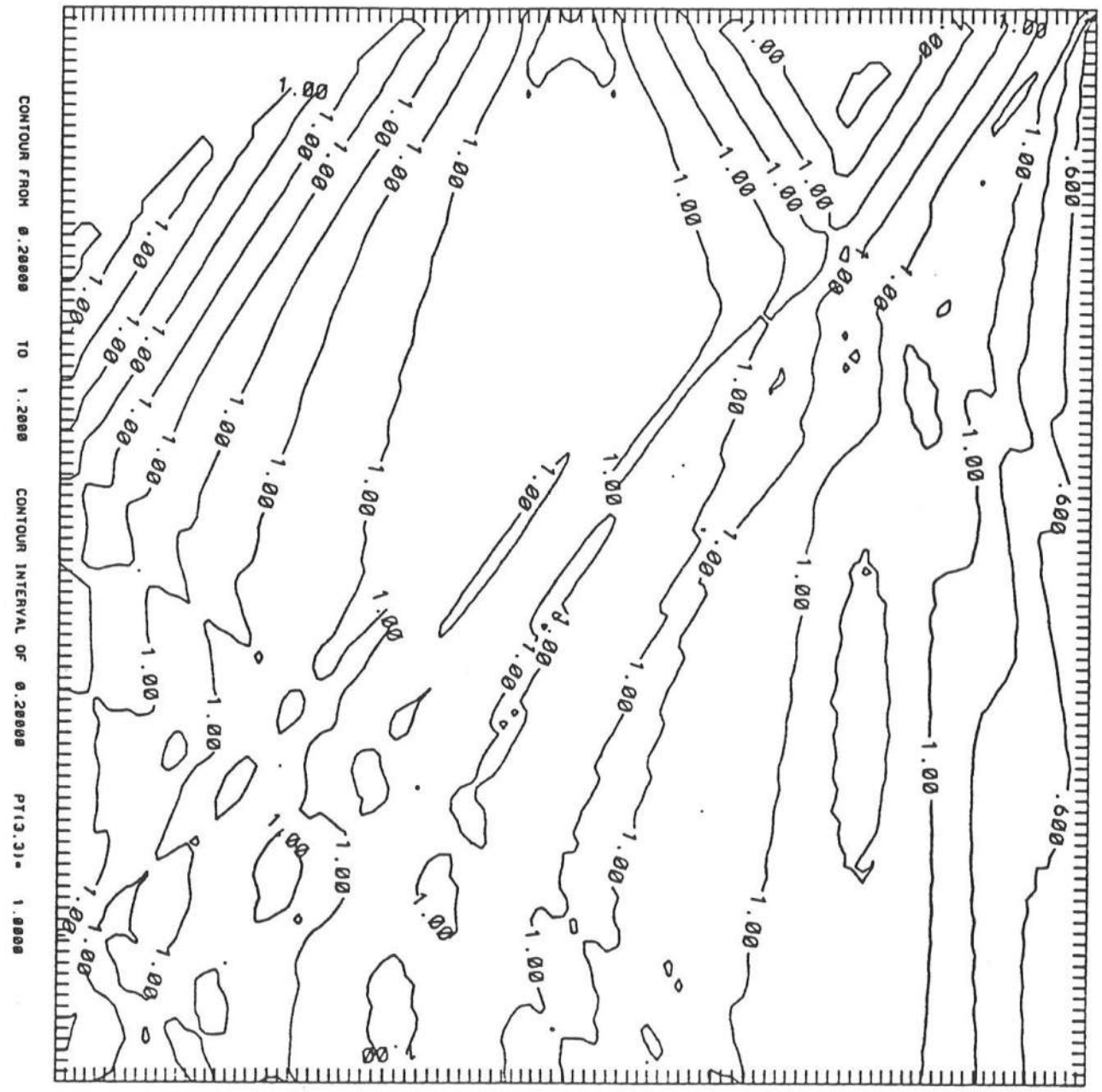

Figure 5: Transmission condition (on left boundary) and diffractive condition (on right boundary) with a normally incident plane wave perturbed by an 'obstacle' on $x = 0$. In (a): density plot of transmission coefficient. In (b): contours of transmission coefficient.

6 Conclusions

Two types of lateral boundary conditions are developed for parabolic water-wave models for diffractive and transmitting boundaries. These conditions are illustrated with a simple parabolic model on constant water depth to demonstrate the validity of the model and the discretization used. In practice, the conditions would be used between a constant-depth region (shadow region) and a variable-depth region (computational domain). Application to variable water depths in both domains is straightforward, through the use of a variable transformation along the boundary as used by Liu & Mei (1976).

A very simple numerical integration is used with the model. For large scale models, it may be that a more accurate boundary integral technique should be used.

Similar lateral boundary conditions are also developed for a two-parameter wide-angle parabolic model. The extension to the three-parameter model discussed by Kirby (1986*a*) can be made, in principle, although the resulting formulae may be too complicated to be useful in practice.

Acknowledgements

R.A.D. was supported in part by the NOAA Office of Sea Grant, Department of Commerce under Grant NA86AA-D-SG040.

References

Ames, W.F. & Lee, D. 1987 Current development in the numerical treatment of ocean acoustic propagation. *Appl. Numer. Math.* **3**, 25–47.

Behrendt, L. 1984 A finite element model for water wave diffraction including boundary absorption and bottom friction. ISVA, Series Paper 37, Tech. Univ. of Denmark, Lyngby.

Booij, N. 1981 Gravity waves on water with non-uniform depth and current. Rpt. 81-1, Dept. of Civil Eng., Delft Univ. of Technology, Delft.

Claerbout, J.F. 1976 *Fundamentals of Geophysical Data Processing.* New York: McGraw-Hill.

Gradshteyn, I.S. & Ryzhik, I.M. 1980 *Table of Integrals, Series and Products.* New York: Academic Press.

Israeli, M. & Orszag, S.A. 1981 Approximation of radiation boundary conditions. *J. Comp. Phys.* **41**, 115–131.

Kirby, J.T. 1986*a* Rational approximations in the parabolic equation method for water waves. *Coastal Engng.* **10**, 355–378.

Kirby, J.T. 1986*b* Open lateral boundary condition for application in the parabolic equation method. *J. Waterway, Port, Coastal & Ocean Eng.*, ASCE **112**, 460–465.

Kirby, J.T. 1989 A note on parabolic radiation boundary conditions for elliptic wave calculations. *Coastal Engng.* **13**, 211–218.

Kirby, J.T. & Dalrymple, R.A. 1983 A parabolic equation for the combined refraction-diffraction of Stokes waves by mildly varying topography. *J. Fluid Mech.* **136**, 453–466.

Larsen, J. & Dancy, H. 1983 Open boundaries in short wave simulations – a new approach. *Coastal Engng.* **7**, 285–297.

Liu, P.L.-F. & Mei, C.C. 1976 Water motions on a beach in the presence of a breakwater. 1. Waves. *J. Geophys. Res.* **81**, 3079–3084.

Marcus, S. W. 1991 A generalized impedance method for application of the parabolic approximation to underwater acoustics. *J. Acoust. Soc. Amer.* **90**, 391–398.

Mei, C.C. 1989 *The Applied Dynamics of Ocean Surface Waves.* Singapore: World Scientific.

Mei, C.C. & Tuck, E.O. 1980 Forward scattering by thin bodies. *SIAM Jl appl. Math.* **39**, 178–191.

Radder, A.C. 1979 On the parabolic equation method for water-wave propagation. *J. Fluid Mech.* **95**, 159–176.

St. Mary, D.F. & Lee, D. 1985 Analysis of an implicit finite difference solution to an underwater wave propagation problem. *J. Comp. Phys.* **57**, 378–390.

Tsay, T.-K. & Liu, P.L.-F. 1982 Numerical solution of water-wave refraction and diffraction problems in the parabolic approximation. *J. Geophys. Res.* **87**, 7932–7940.

Appendix. Exact solution in the shadow region

Consider the 'shadow region', $x > 0$, $y > y_b$. We shall solve the simple parabolic equation (1.3) and the wide-angle parabolic equation (1.4) exactly within this region, subject to appropriate boundary conditions.

Simple parabolic equation

We consider

$$\frac{\partial^2 A}{\partial y^2} + \pi\Omega^2 \frac{\partial A}{\partial x} = 0 \qquad \text{(A 1)}$$

subject to the boundary conditions

$$A(x, y_b) = A_b(x) \quad \text{for } x > 0 \qquad \text{(A 2)}$$

and

$$A(0, y) = 0 \quad \text{for } y > y_b, \qquad \text{(A 3)}$$

where $A_b(x)$ is assumed known and

$$\Omega^2 = 2ik/\pi; \qquad \text{(A 4)}$$

we also assume that

$$A(x,y) \text{ is bounded as } y \to \infty. \tag{A 5}$$

Clearly, the solution is a function of $(y - y_b)$, so, without loss of generality, we can set $y_b = 0$.

We note that, due to the assumption (1.2), (A 3) is a comparable approximation to $\partial\phi/\partial x = 0$ on $x = 0$, which is itself the appropriate boundary condition on a rigid wall or impermeable breakwater.

We solve for A using a Laplace transform in x (other methods could be used; see Marcus (1991) for an alternative derivation):

$$\mathcal{L}\{A\} \equiv \overline{A}(p,y) = \int_0^\infty A(x,y)\,\mathrm{e}^{-px}\,dx,$$

where we suppose that $\mathrm{Re}\,p > 0$. Since

$$\mathcal{L}\left\{\frac{\partial A}{\partial x}\right\} = p\overline{A}(p,y) - A(0,y) = p\overline{A}(p,y),$$

by (A 3), the partial differential equation (A 1) is transformed into

$$\frac{\partial^2 \overline{A}}{\partial y^2} + \pi p \Omega^2 \overline{A} = 0,$$

with general solution

$$\overline{A}(p,y) = C(p)\exp\{\mathrm{i}y\Omega\sqrt{\pi p}\} + D(p)\exp\{-\mathrm{i}y\Omega\sqrt{\pi p}\}.$$

Given (A 4), we define Ω by

$$\Omega = (1+\mathrm{i})\sqrt{(k/\pi)}.$$

Then, (A 5) implies that $D(p) \equiv 0$, whence (A 2) gives $C(p) = \overline{A_b}(p)$. Hence,

$$\overline{A}(p,y) = \overline{A_b}(p)\exp\{(-1+\mathrm{i})y\sqrt{kp}\}. \tag{A 6}$$

This formula can be inverted using the convolution theorem, namely

$$\mathcal{L}\{u\}\mathcal{L}\{v\} = \mathcal{L}\left\{\int_0^x u(x-\xi)v(\xi)\,d\xi\right\}.$$

From Gradshteyn & Ryzhik (1980, §17.13, Eq. (32)), with a little manipulation, we have

$$\exp\{\mathrm{i}y\Omega\sqrt{\pi p}\} = \mathcal{L}\left\{-\frac{\mathrm{i}y\Omega}{2x^{3/2}}\exp\left(\frac{\pi\Omega^2 y^2}{4x}\right)\right\}. \tag{A 7}$$

Hence, the convolution theorem gives

$$A(x,y) = -\frac{1}{2}\mathrm{i}y\Omega\int_0^x \frac{A_b(\xi)}{(x-\xi)^{3/2}}\exp\left\{\frac{\mathrm{i}ky^2}{2(x-\xi)}\right\}d\xi. \tag{A 8}$$

Despite appearances, this function is indeed small for large y; in fact, an integration by parts shows that, as $y \to \infty$,

$$A(x,y) \sim \frac{2\mathrm{i}x^{1/2}}{\pi\Omega y}A_b(0)\exp\left\{\frac{\mathrm{i}ky^2}{2x}\right\} + O(y^{-3}).$$

If we differentiate (A 6) with respect to y, we obtain

$$\frac{\partial \overline{A}(p,y)}{\partial y} = \mathrm{i}\Omega\sqrt{\pi p}\,\overline{A}(p,y) = \mathrm{i}\Omega\sqrt{(\pi/p)}\,\{p\overline{A}(p,y)\}.$$

Using the convolution theorem again, we deduce that

$$\frac{\partial A(x,y)}{\partial y} = \mathrm{i}\Omega\int_0^x \frac{\partial A(\xi,y)}{\partial \xi}\,\frac{d\xi}{\sqrt{x-\xi}}; \tag{A 9}$$

in particular, on $y = 0$,

$$\frac{\partial A(x,0)}{\partial y} = \mathrm{i}\Omega\int_0^x \frac{A_b'(\xi)}{\sqrt{x-\xi}}\,d\xi. \tag{A 10}$$

This equation is the starting point for the derivation in §3 of the generalized impedance boundary condition.

Wide-angle parabolic equation

We consider (1.4), subject to the same boundary conditions as before, namely (A 2), (A 3) and (A 5); again, we can set $y_b = 0$. We find that $\overline{A}$ satisfies

$$\frac{\partial^2 \overline{A}}{\partial y^2} + \gamma^2\overline{A} = 0,$$

where

$$\gamma^2 = \frac{pk^2}{\beta(p-2\mathrm{i}\lambda)} \qquad \text{and} \qquad \lambda = \frac{k\alpha}{2\beta} > 0;$$

hence.

$$\overline{A}(p,y) = C(p)\mathrm{e}^{\mathrm{i}\gamma y} + D(p)\mathrm{e}^{-\mathrm{i}\gamma y}.$$

We choose the square root so that $\mathrm{Re}\,\gamma > 0$, whence $D \equiv 0$, $C(p) = \overline{A_b}(p)$ and

$$\overline{A}(p,y) = \overline{A_b}(p)\mathrm{e}^{\mathrm{i}\gamma y}.$$

Differentiating with respect to y gives

$$\frac{\partial \overline{A}(p,y)}{\partial y} = \frac{\mathrm{i}\gamma}{p}\,\{p\overline{A}(p,y)\}.$$

If we write

$$\gamma/p = k\beta^{-\frac{1}{2}}\,\mathcal{L}\{w\},$$

say, the convolution theorem gives (cf. (A 9))

$$\frac{\partial A(x,y)}{\partial y} = \frac{\mathrm{i}k}{\sqrt{\beta}}\int_0^x w(x-\xi)\,\frac{\partial A(\xi,y)}{\partial \xi}\,d\xi.$$

To find w, we use the convolution theorem again:

$$\mathcal{L}\{w\} = p^{-\frac{1}{2}}(p-2\mathrm{i}\lambda)^{-\frac{1}{2}} = \pi^{-1}\mathcal{L}\{x^{-\frac{1}{2}}\}\,\mathcal{L}\{x^{-\frac{1}{2}}\mathrm{e}^{2\mathrm{i}\lambda x}\},$$

whence

$$w(x) = \frac{1}{\pi}\int_0^x \frac{e^{2i\lambda\xi}}{\sqrt{\xi}\sqrt{x-\xi}}\,d\xi.$$

To evaluate this integral, set $\xi = x\sin^2(\theta/2)$ giving

$$\begin{aligned} w(x) &= \frac{1}{\pi}\int_0^{\pi} \exp\{2i\lambda x \sin^2(\theta/2)\}\,d\theta \\ &= \frac{1}{2\pi}e^{i\lambda x}\int_{-\pi}^{\pi} e^{-i\lambda x\cos\theta}\,d\theta = e^{i\lambda x}J_0(\lambda x). \end{aligned}$$

Substituting for w and setting $y = 0$ now gives

$$\frac{\partial A(x.0)}{\partial y} = \frac{ik}{\sqrt{\beta}}\int_0^x A_b'(\xi)\,e^{i\lambda(x-\xi)}J_0(\lambda(x-\xi))\,d\xi, \qquad \text{(A 11)}$$

which is a generalization of (A 10); this formula is used in §5.

List of Figures